

# “Time-Reversal Measurement of the p-Wave Cross Sections of the ${}^7\text{Be}(n,\alpha){}^4\text{He}$ Reaction for the Cosmological Li Problem”

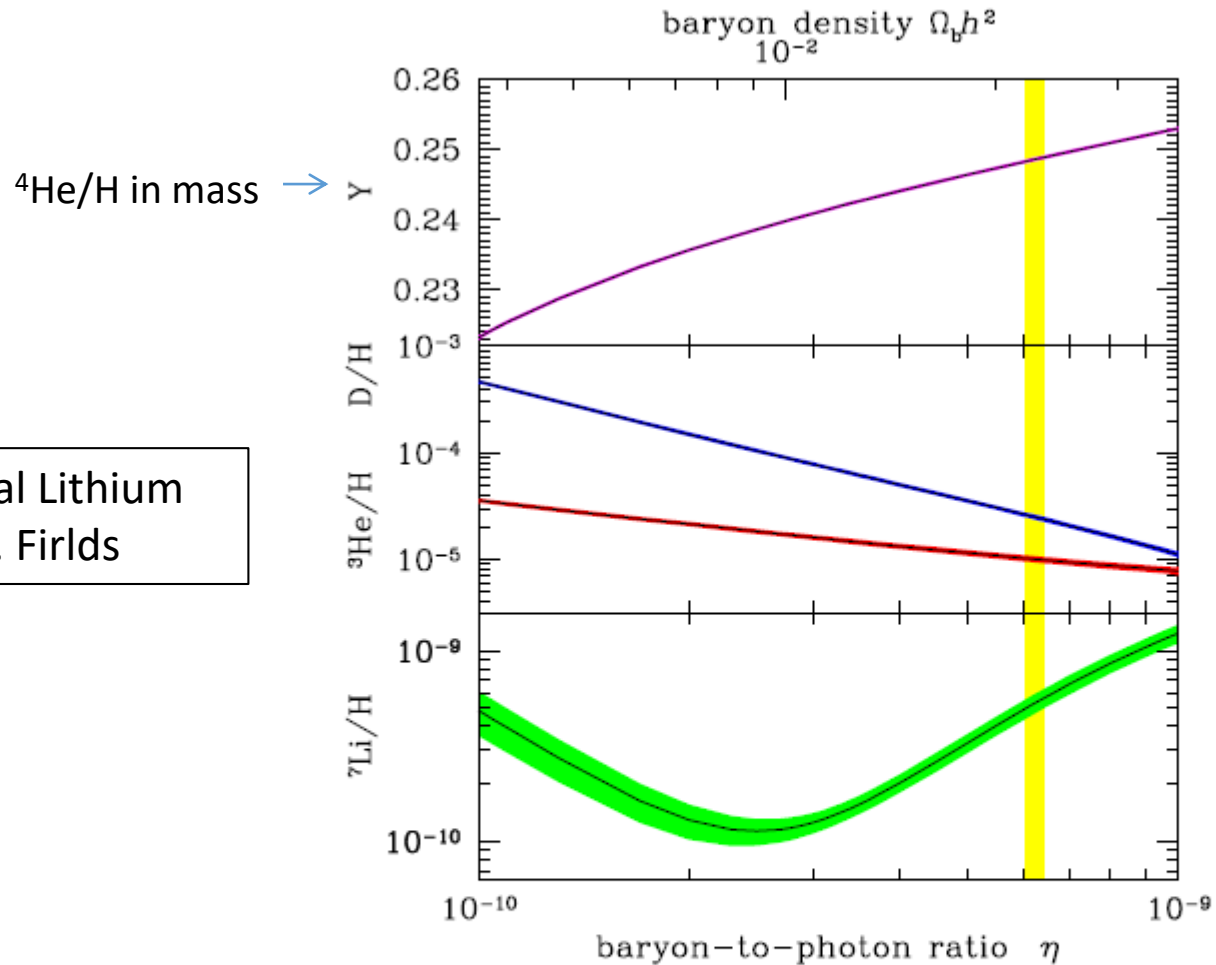
T. Kawabata et. al., PRL 118, 052701 (2017)

# Lithium Problem

Usually, the term “Lithium problem” means , , ,

1. Mismatch of the abundance of  ${}^7\text{Li}$  between observations and Big bang nucleosynthesis (BBN) theory estimation
2. Discrepancy of the ratio  ${}^7\text{Li}/{}^6\text{Li}$  estimated from BBN

# Big Bang Theory prediction of each abundance



From “The Primordial Lithium Problem” , Brian D. Fields

Figure 2: BBN theory predictions for light nuclide abundances vs baryon-to-photon ratio  $\eta$ . Curve widths:  $1\sigma$  theoretical uncertainties. Vertical band: WMAP determination of  $\eta$ .

# Comparison of ${}^7\text{Li}$ abundance with prediction

Corresponds to  ${}^7\text{Li}/\text{H} \rightarrow$

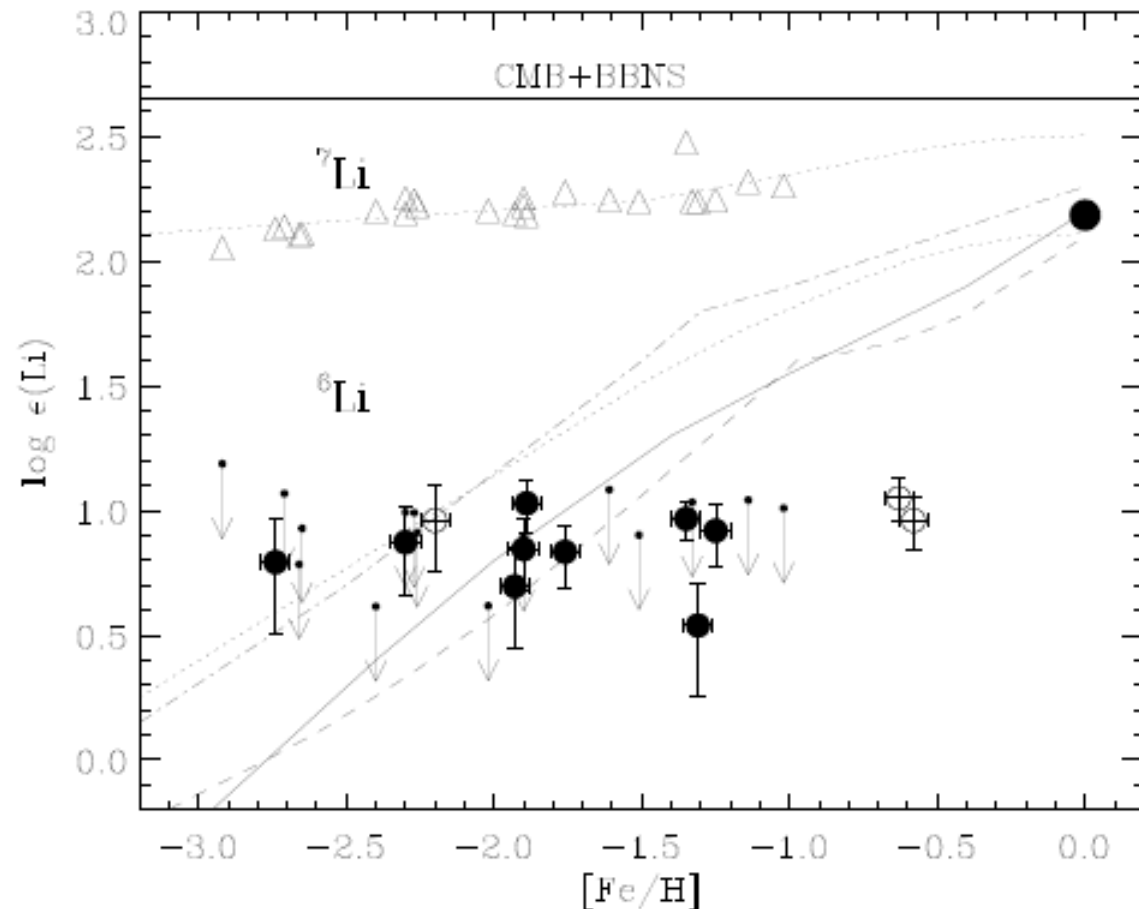


Figure 3: Lithium abundances in selected metal-poor Galactic halo stars, from (46) with permission. For each star, elemental  $\text{Li} = {}^6\text{Li} + {}^7\text{Li}$  is plotted at the star's metallicity  $[\text{Fe}/\text{H}] = \log_{10}[(\text{Fe}/\text{H})_{\text{obs}}/(\text{Fe}/\text{H})_{\odot}]$ . The flatness of  $\text{Li}$  vs  $\text{Fe}$  is the “Spite plateau” and indicates that the bulk of the lithium is unrelated to Galactic nucleosynthesis processes and thus is primordial. The horizontal band gives the BBN+WMAP prediction; the gap between this and the plateau illustrates the  ${}^7\text{Li}$  problem. Points below the plateau show  ${}^6\text{Li}$  abundances; the apparent plateau constitutes the  ${}^6\text{Li}$  problem.

# Reference : $^7\text{Li}$ abundance

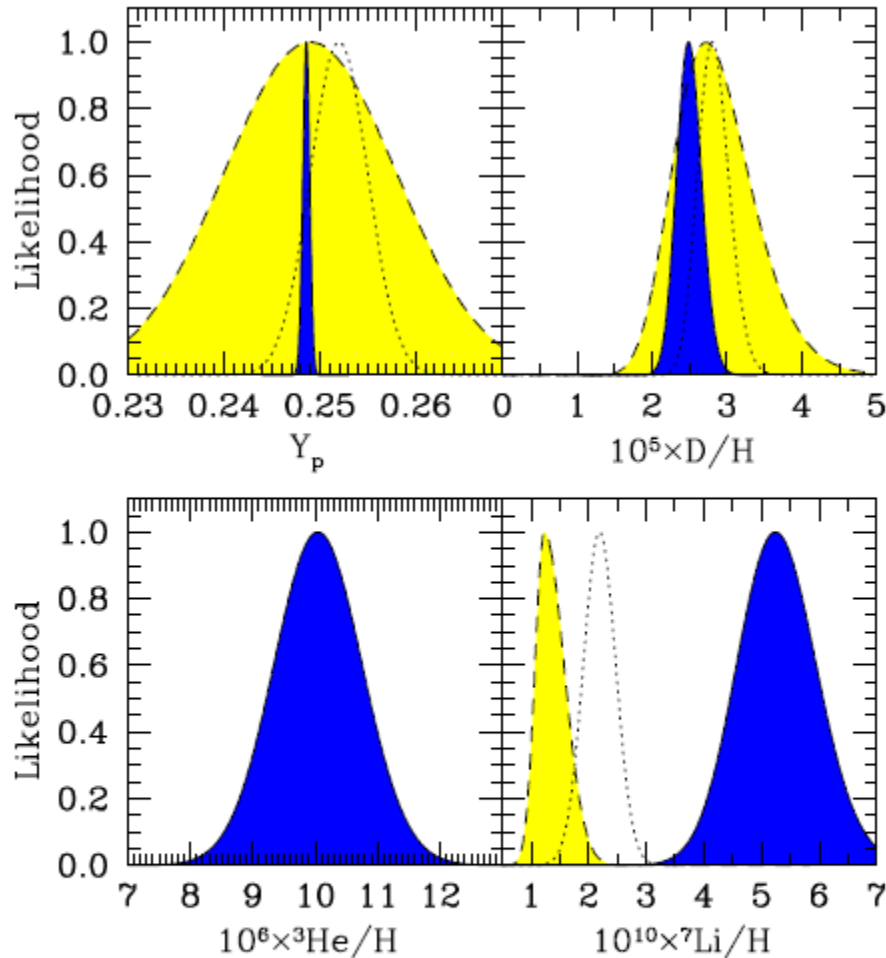


FIG. 4: The theoretical and observational likelihood functions for  $^4\text{He}$ ,  $D/H$ ,  $^3\text{He}/H$ , and  $^7\text{Li}/H$ . BBN results have been convolved with the WMAP determination of  $\eta$  and are shown as dark (blue) shaded area. The observational likelihoods are shown as light (yellow) shaded regions as well as alternative dotted curves. The data and distinctions are detailed in the text.

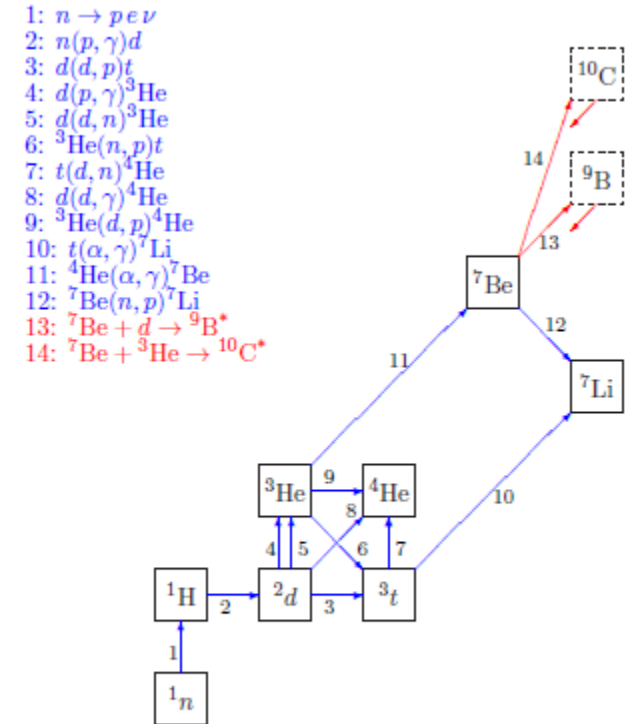


Figure 1: Simplified BBN nuclear network: 12 normally imp shown in blue, and proposed/tested new reactions in red.

# Motivation

From a view of nuclear physics, nuclear-reaction rates involved in the BBN theory should be examined. The main process of the  ${}^7\text{Li}$  production in the BBN is the electron-capture decay of  ${}^7\text{Be}$ , which is synthesized in the  ${}^3\text{He}({}^4\text{He}, \gamma){}^7\text{Be}$  reaction. Direct measurements of the cross section for the  ${}^3\text{He}({}^4\text{He}, \gamma){}^7\text{Be}$  reaction were extensively carried out in the past by several groups, and uncertainties in this thermonuclear reaction rate are now very small. There is no room to modify the  ${}^7\text{Be}$  production rate to solve the lithium problem [7].

Recently, it was pointed out that the  ${}^7\text{Li}$  abundance will be greatly reduced in the BBN calculation if the destruction rate of  ${}^7\text{Be}$  is enhanced. One of the candidate channels to destruct  ${}^7\text{Be}$  is the  ${}^7\text{Be}(n, \alpha){}^4\text{He}$  reaction.

# ${}^7\text{Be}(n,\alpha){}^4\text{He}$ Reaction and the Cosmological Lithium Problem: Measurement of the Cross Section in a Wide Energy Range at n\_TOF at CERN

M. Barbagallo, et. al., PRL 117, 152701 (2016)

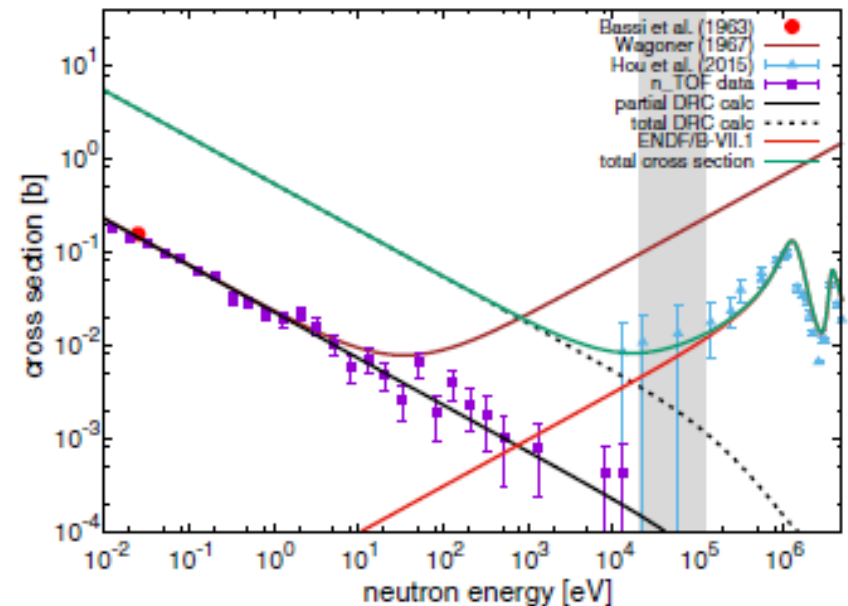
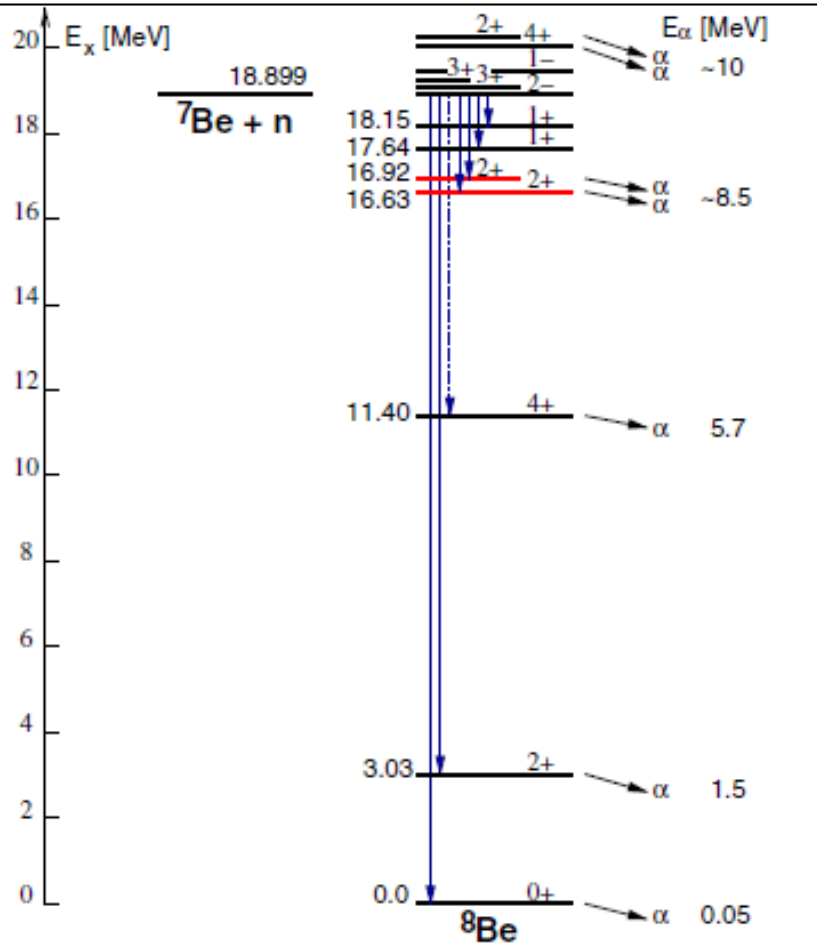


FIG. 3. The partial  ${}^7\text{Be}(n, \gamma\alpha)$  cross section measured at n\_TOF between 10 meV and 10 keV (blue squares), compared with the result of Bassi *et al.* [12] at thermal energy (red circle). The solid lines represent the total DRC calculation.

***Precedent experiment & result***

# Experiment

- Beam line in RCNP (Osaka, Japan)
- Using inverse reaction  ${}^4\text{He}(\alpha, n){}^7\text{Be}$
- Target He (gas) irradiated by He beam with energy of  $\sim 40$  MeV
- Scattered neutron is measured by liquid scintillation counter



# Neutron Energy spectrum

The spectrum is obtained from liquid scintillator (BC-501A).  
(neutron vs gamma event selection is necessary ..... )

Subtraction of empty target run

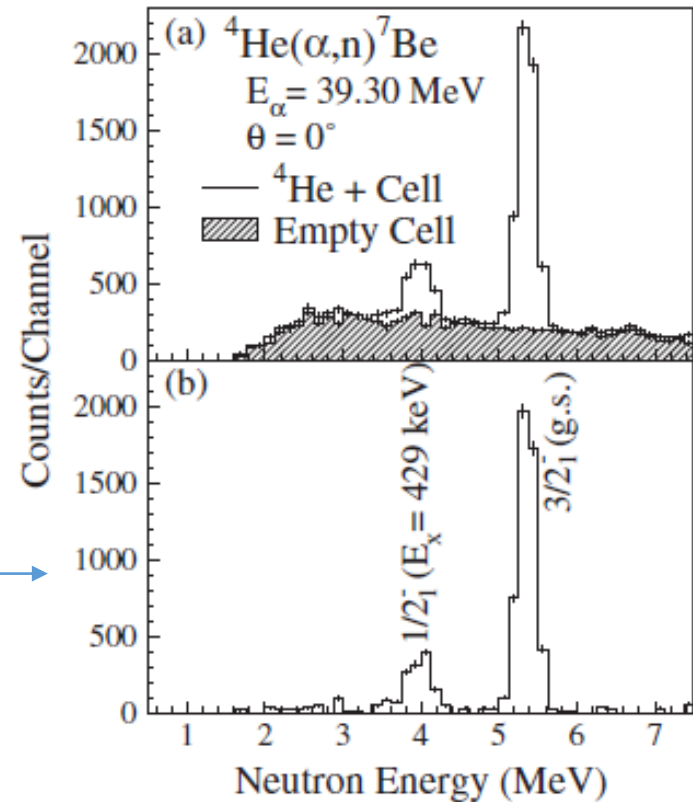


FIG. 1. Neutron energy spectra in the  $^4\text{He}(\alpha, n)^7\text{Be}$  reaction measured at  $E_\alpha = 39.30 \text{ MeV}$  and  $\theta_{\text{lab}} = 0^\circ$ . (a) Open and hatched spectra were taken using the He gas-filled and empty cells, respectively. (b) Background-free spectrum obtained by subtracting the background spectrum taken from the empty-cell measurement.

# Cross section

## Angular distribution

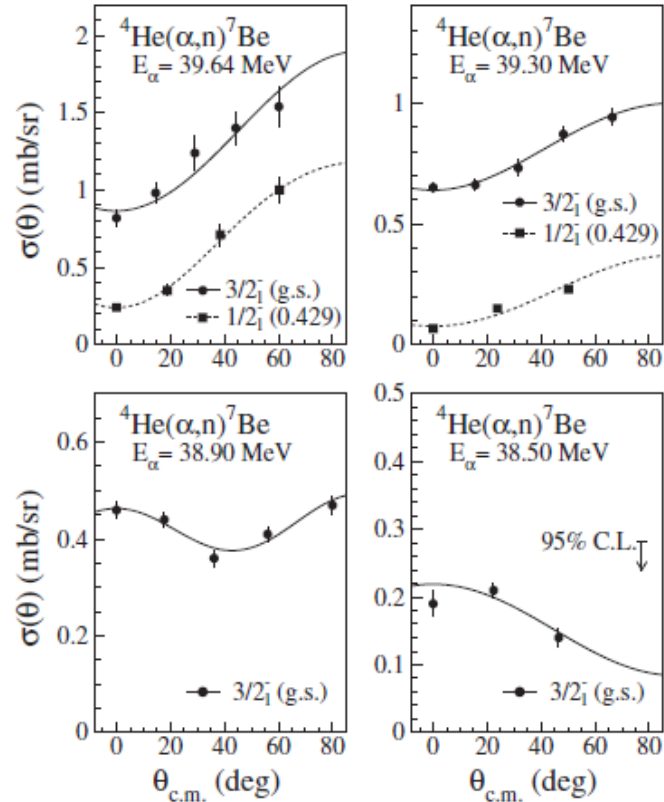


FIG. 2. Angular distribution of the differential cross sections for the  $^4\text{He}(\alpha, n)^7\text{Be}$  reaction. The solid circles and squares show the differential cross sections for the ground and first excited states in  $^7\text{Be}$ , respectively. The solid and dashed lines are series of the even-order Legendre polynomials to fit the experimental data.

## Total cross section

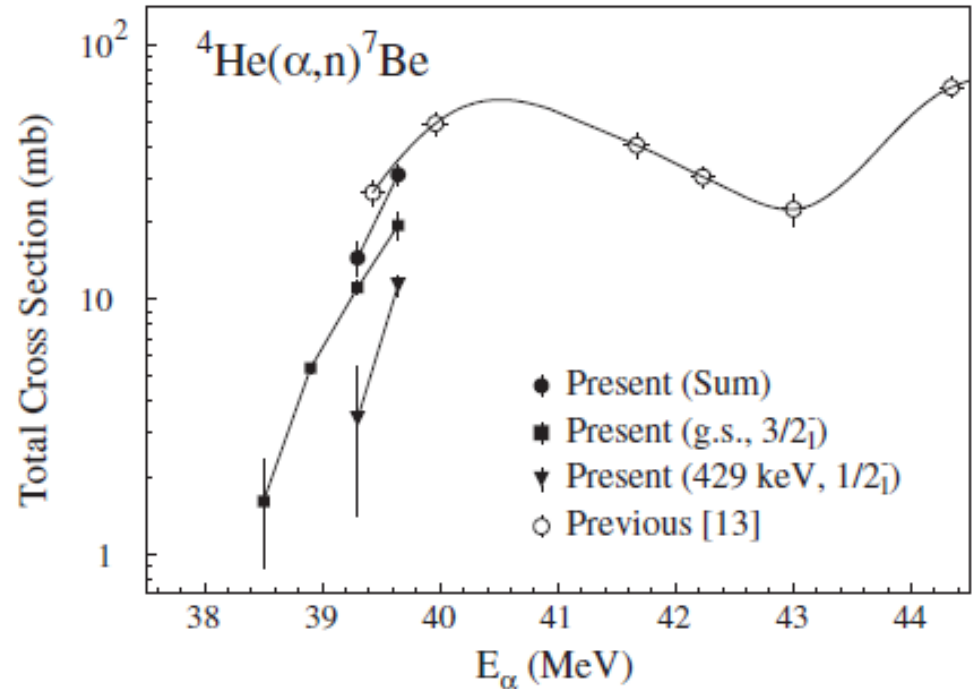


FIG. 3. Measured total cross sections of the  $^4\text{He}(\alpha, n)^7\text{Be}$  reaction for the ground (solid squares) and first excited (solid triangles) states. The sum of the two states is shown by solid circles. Previous results from Ref. [13] are shown by the open circles. The solid lines interpolating the data points are drawn for a guide to the eye.

# Comparison with the other result/theoretical estimation

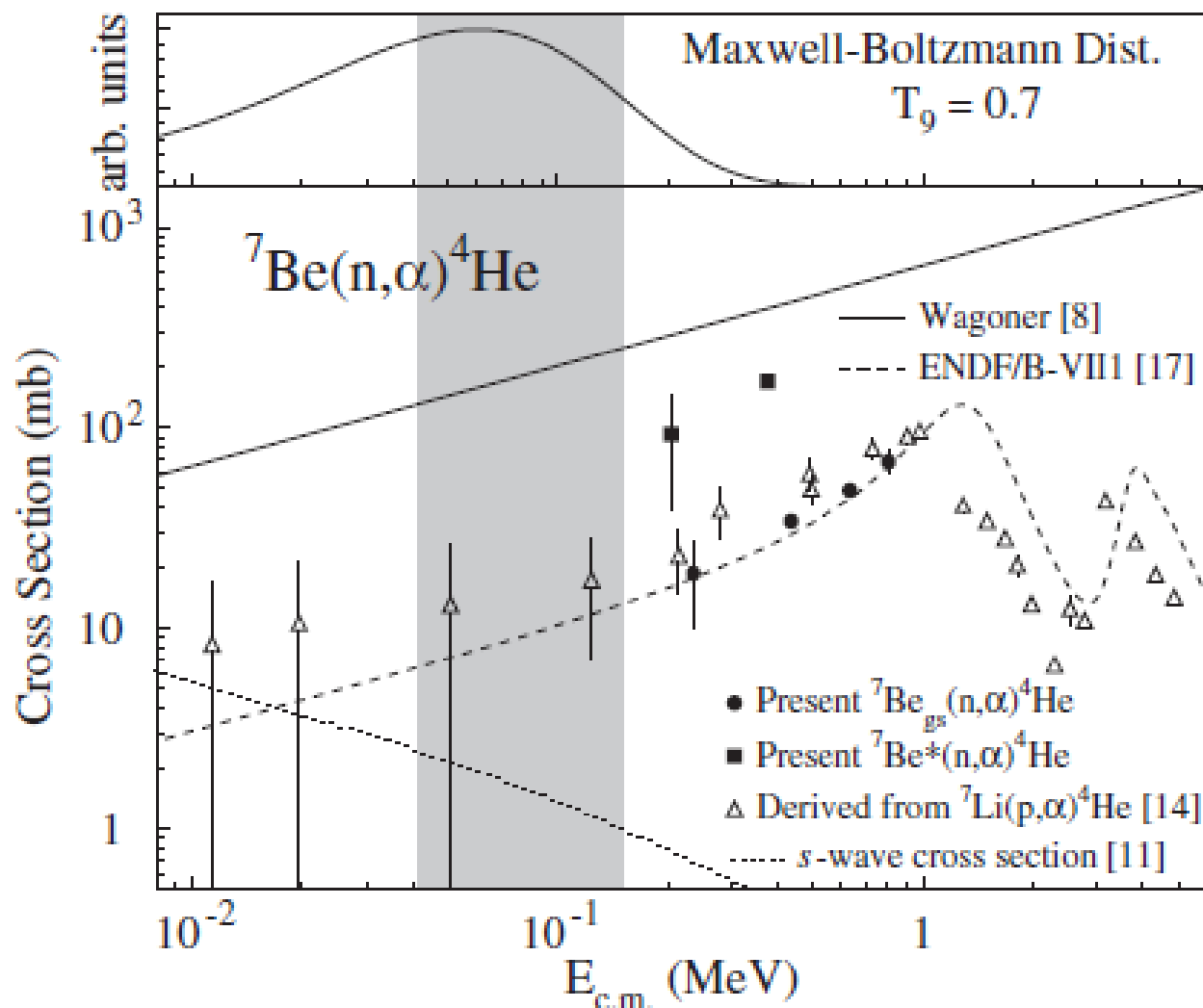


FIG. 4. Measured total cross sections for the  ${}^7\text{Be}(n, \alpha){}^4\text{He}$  reaction on the ground (solid circles) and first excited (solid squares) states. The cross sections for the first excited state are